Low Speed Position Estimation Scheme for Model Predictive Control with Finite Control Set

Shamsuddeen Nalakath*, Matthias Preindl†, Nahid Mobarakeh Babak‡ and Ali Emadi*
*Department of Electrical and Computer Engineering
McMaster University, Hamilton, Ontario, Canada
†Department of Electrical Engineering
Columbia University in the City of New York
‡Institut National Polytechnique de Lorraine,Vandoeuvre-Les-Nancy, France

***Abstract*—This paper presents the low speed position estimation scheme for an IPM machine controlled by model predictive control with finite control set. The career signal injection is not viable as there is no PWM to superimpose it with PWM for this type of control. The pulse vector injection technique requires current derivative sensors which makes the overall scheme less attractive. This paper utilizes the inherent high frequency vector injection of the model predictive control to extract the position information. It is shown that the high frequency current response is amplitude modulated with respect to the position. A demodulation technique based on the reactive power estimation is proposed. The simulation results at various initial positions confirm the validity of the proposed position estimation scheme.**

I. Introduction

The simplest and widely used industrial technique for controlling AC induction motor is v/f control. This technique has slow dynamic responses and it lacks steady state accuracy mainly due to the fact that the torque and flux are not directly controlled. The independent control of torque and flux producing current components in dq frame for field oriented control (FOC) technique overcomes these drawbacks. However, the cascaded current and speed PI controllers in FOC may slows down the dynamics especially if they are not well tuned. The torque is directly controlled by controlling the magnitude and direction of flux vector in direct torque control (DTC). By exploiting high flux dynamics and as the control is realized by hysteresis controllers and switching table, the torque response of DTC is much faster than FOC. In contrast to the FOC realized by PWM, DTC has higher ripple currents.

Even though the model predictive control (MPC) was originally developed for process industries with a very slow sampling rate, it has been recently started applying in power electronics and motor drives applications with the help of modern fast processors [1]. The MPC predicts the control input sequence which minimizes the cost function over a prediction horizon. The first input of the predicted sequence is only applied to the plant at the current sampling time and then the process is repeated for entire sampling times. The control sequence is predicted offline in explicit MPC and online in implicit MPC [2]. The memory requirement to store the control input for the entire operating period is the main drawback of the explicit MPC. The minimization of cost function is a nonlinear optimization problem, and therefore the computational requirement to solve online is the main challenge in implicit MPC [2].

The continuous MPC mentioned in the previous paragraph predicts the input sequence form the infinite possibilities. In contrast, the control input sequence corresponding to minimum cost function is chosen from the set of possible sequences for the case of MPC with finite control set (FCS) [2][3]. The possible sequences are based on the switching states of the inverter in the case of MPC for motor drives. The computational requirement is less for MPC with FCS that makes it a best candidate for online optimization. The MPC with FCS is applied to control torque and flux components in $\alpha\beta$ reference frame like in DTC is known as MPDTC [4][5][6]. The torque and flux errors with respect to their reference and predicted values are minimized in the form of a cost function. The position information is required if the MPC is carried out in dq reference frame unlike the case of $\alpha\beta$ frame. The control in dq frame is convenient for online optimization as the associated mathematical models becomes simpler. The optimized operation with MTPA and minimum loss can be incorporated in MPC by adding the corresponding terms in the cost function [7].

The position estimation is carried out differently for low and high speeds. The low speed position estimation is done by exploiting magnetic nonlinearities in the electromagnetic structure (saturation, saliency, slot harmonics, etc). The back emf is utilized for the position estimation at high speed. The signal injection methods are the most reliable approach available so far at low speeds [8]. The sinusoidal or square wave high frequency signals are injected at dq or $\alpha\beta$ frame. The first one is known as pulsating injection and the second one is rotating injection. The PWM is used to superimpose the high frequency signals to the fundamental excitation. The high frequency responses of the signals are modulated by magnetic nonlinearities. The nonlinearities are position dependent. Therefore with a proper demodulation technique the position information can be extracted. The saliency of the rotor is exploited for the position estimation of the interior permanent magnet motors. The saliency dependent inductance varies double as the frequency of the fundamental. Hence exists a π ambiguity in the position estimation [8]. The polarity detection is used to compensate for this ambiguity [8][9].

978-1-5090-3474-1/16/$31.00 ©2016 IEEE

The high frequency signal injection is not compatible with MPC with FCS as there is no PWM to superimpose the high frequency signal with the fundamental excitation.

The pulse vector injection applies sequential positive and negative pulse vectors by modifying the fundamental PWM [8][10]. One of the most popular pulse vector injection technique is indirect flux detection by online reactance measurement (INFORM) [11]. The three space voltage vectors and their corresponding negative vectors are applied sequentially over three PWM cycles. The current derivative responses from all the three phases are processed to get the position information. The PWM responses without any modification is also used estimate the position [8]. This technique doesn't have any additional current ripple due to injection. The pulse vector injection can be integrated with fundamental excitation vectors of MPC with FCS to estimate the position. As there is no PWM to synchronize pulse vector injection in MPC with FCS, it has to be applied sequentially with a fixed frequency. The current ripple and requirement of current derivative sensors makes this scheme less attractive.

The MPC with FCS applies six active voltage vectors of a two level inverter in accordance with the vector which produce minimum cost function. The frequency of the vectors is varying and always much higher than the fundamental frequency. The high frequency voltage vectors produce arbitrary current response. The amplitude of the responses is modulated with the position. The position information can be extracted from the high frequency response with a proper demodulation technique. This paper analyzes the high frequency response and also proposes a demodulation technique based on the reactive power estimation. The section II presents the MPC with finite control set. The position estimation scheme is described in section III. The simulation results and conclusion of the work are presented in sections IV and V respectively.

II. Model Predictive Control with Finite Control Set

The MPC with FCS chooses a sequence corresponding to minimum cost function from all the possible switching sequence of a two level inverter. A sequence consists of switching states in accordance with the possible transition. The possible switching transitions of a two level inverter is given in Fig. 1.

The cost functions for all the possible sequences corresponding to the last switching state are computed for a given prediction horizon N at the current sampling time. The first input of the sequence which produces minimum cost function is only applied to the plant in the next sampling time. This process is repeated for the entire sampling intervals and Fig. 2 illustrates the process.

The MPC with FCS can be used to control torque and flux, and operate at MTPA and minimum loss by adding the appropriate terms in the cost function. The currents id and iq are controlled in this work. Then, the cost function would be the error between the reference and measured feedback of id and iq. The prediction horizon is chosen as $N = 1$.

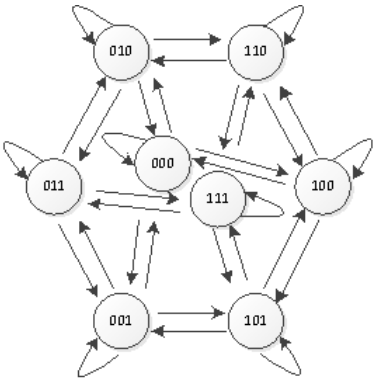

Fig. 1: Admissible switching transitions of a two level inverter.

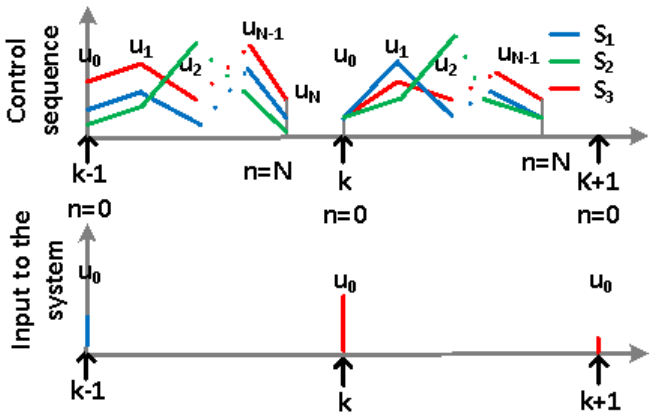

Fig. 2: Illustration of MPC with FCS (N- prediction horizon, s-sequences, u- control input/switching states, and k- sampling time).

The general motor control scheme with MPC with FCS is given in Fig. 3. The measurement delay for the currents is compensated by estimating the current from the machine model. The sequence selector selects the possibles switching states based on the previous state. A sequence has only one input as $N = 1$. The switching state which produces minimum cost function is chosen as the control input by the cost minimization block. The selected control input is then applied to the machine at the current sampling time.

III. Position Estimation Scheme

The voltage vectors which are applied to the electric machine by MPC with FCS are

$$V_n = \begin{bmatrix} V_a \\ V_b \\ V_c \end{bmatrix} \quad ; \quad n = 0 - 7 \tag{1}$$

where V_n is the voltage vector, and V_a, V_b and V_c are its abc phase components. The subscript n indicates the voltage vector corresponding to six active and two null switching states. The vector diagram showing all the states is given in Fig. 4.

The estimated dq axes rotates with an angle θ_e from the stationary axis. It has angle offset of $\Delta\theta$ from the actual dq

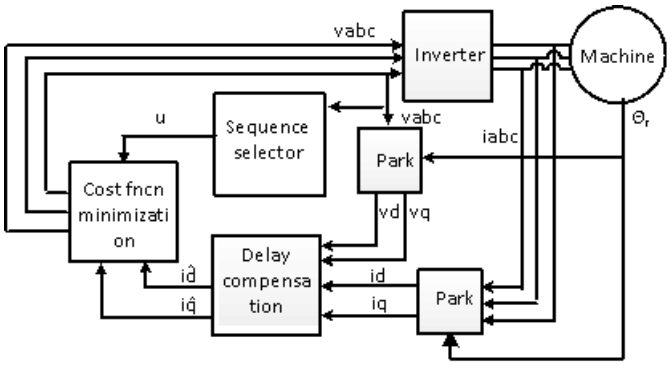

Fig. 3: MPC with FCS control scheme.

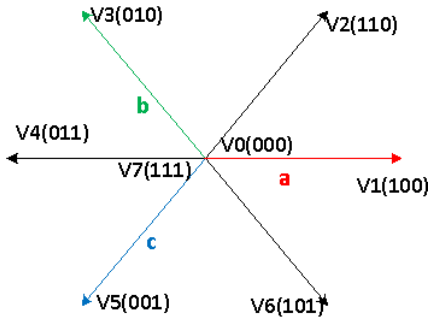

Fig. 4: Voltage vectors.

axes as shown in Fig. 5. The voltage vectors in estimated dq axes is

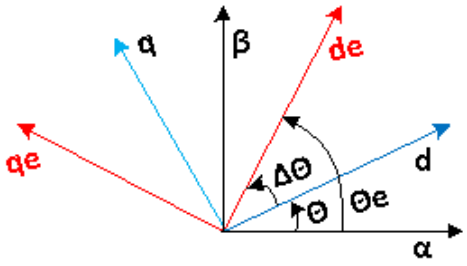

Fig. 5: Actual and estimated dq axes.

$$\begin{bmatrix} v_{de} \\ v_{qe} \end{bmatrix} = \frac{2}{3} \begin{bmatrix} cos(\theta_e) & cos(\theta_e - \frac{2\pi}{3}) & cos(\theta_e + \frac{2\pi}{3}) \\ sin(\theta_e) & sin(\theta_e - \frac{2\pi}{3}) & sin(\theta_e + \frac{2\pi}{3}) \\ \frac{1}{2} & \frac{1}{2} & \frac{1}{2} \end{bmatrix} \begin{bmatrix} V_a \\ V_b \\ V_c \end{bmatrix} \quad (2)$$

The voltage vectors in actual dq axes is

$$\begin{bmatrix} v_d \\ v_q \end{bmatrix} = \begin{bmatrix} cos(\Delta\theta) & sin(\Delta\theta) \\ -sin(\Delta\theta) & cos(\Delta\theta) \end{bmatrix} \begin{bmatrix} v_{de} \\ v_{qe} \end{bmatrix} \quad (3)$$

The voltages V_{dq} has fundamental DC (at steady state) and high frequency components. The latter component results in high frequency current response. In the high frequency response, the inductance effect is much dominant as compared to the resistance and hence it is usually neglected. The cross coupling and back emf terms are also negligible as the speed is low or at standstill. Consequently, the high frequency machine model becomes

$$\begin{bmatrix} v_{dh} \\ v_{qh} \end{bmatrix} = \begin{bmatrix} L_d & 0 \\ 0 & L_q \end{bmatrix} p \begin{bmatrix} i_{dh} \\ i_{qh} \end{bmatrix} \quad (4)$$

The high frequency current response from (4) can be found as

$$\begin{bmatrix} i_{dh} \\ i_{qh} \end{bmatrix} = \int \begin{bmatrix} v_d/L_d \\ v_q/L_q \end{bmatrix} dt \quad (5)$$

The current response in estimated dq axes is

$$\begin{bmatrix} i_{deh} \\ i_{qeh} \end{bmatrix} = \begin{bmatrix} cos(\Delta\theta) & -sin(\Delta\theta) \\ sin(\Delta\theta) & cos(\Delta\theta) \end{bmatrix} \begin{bmatrix} i_{dh} \\ i_{qh} \end{bmatrix} \quad (6)$$

$$= \begin{bmatrix} v_{deh}(\frac{cos^2(\Delta\theta)}{L_d} + \frac{sin^2(\Delta\theta)}{L_q}) + v_{qeh}cos(\Delta\theta)sin(\Delta\theta)(\frac{1}{Ld} - \frac{1}{Lq}) \\ v_{qeh}(\frac{cos^2(\Delta\theta)}{L_q} + \frac{sin^2(\Delta\theta)}{L_d}) + v_{deh}cos(\Delta\theta)sin(\Delta\theta)(\frac{1}{Ld} - \frac{1}{Lq}) \end{bmatrix} \quad (7)$$

The high frequency response currents i_{dqeh} is modulated with the position. The standard demodulation techniques used for carrier signal injection cannot be implemented for this scheme. The main reason is that the high frequency voltage component is an arbitrary waveform. The demodulation by estimating reactive power is proposed in this paper. The high frequency reactive power is

$$q_{he} = v_{deh}i_{qeh} - v_{qeh}i_{deh} \quad (8)$$

$$= v_{de}v_{qe}(\frac{1}{L_q} - \frac{1}{L_d}) + sin(2\Delta\theta)(\frac{1}{L_d} - \frac{1}{L_q})(v_{deh}^2 - v_{qeh}^2) \quad (9)$$

The first part of (9) is high frequency component which can be eliminated by a LPF. The second part becomes zero if the $L_d = L_q$. Therefore this technique can be used only for IPM. The term $sin(2\Delta\theta)$ becomes $2\Delta\theta$ when $\Delta\theta \cong 0$. Therefore, a linear observer like PLL can be used to estimate the position constantly.

The complete demodulation scheme is presented in Fig. 6. The estimated dq axes components of current measurement (i_{dqe}) are passed through a LPF to get fundamental components (i_{dqef}) . Then, i_{dqef} is subtracted from i_{dqe} to get high frequency components (i_{dqeh}). The high frequency voltage components v_{dqeh} are also found in the similar way. Then, the reactive power is found (q_{eh}) by multiplying respective voltage and current components. The output of LPF by passing q_{eh} is $sin(2\Delta\theta)$ which is fed to PLL. The PLL output is speed and the estimated position is found by integration.

IV. Simulation Results

The simulation is carried out in MATLAB Simulink to analyze and validate the proposed position estimation scheme. The reference IPM parameters used for simulation is given in Table I. The operating condition used for simulation is i_q = 1.25 A, i_d = 0 A, θ_{ini}= 0^o, ω= 40 rad/s (elec), unless otherwise is mentioned.

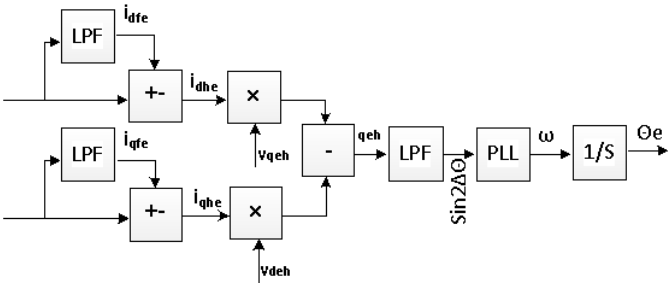

Fig. 6: Demodulation scheme.

TABLE I: IPM Parameters

DC link voltage	300 V
Phase resistance	0.4 Ω
d-axis inductance	10.2 mH
q-axis inductance	12.8 mH

The voltage vectors in estimated dq axes is shown in Fig. 7. These voltages have both the fundamental DC and high frequency terms as shown in Fig. 8. It is seen that the high frequency voltage component is fairly well enough to create high frequency current response.

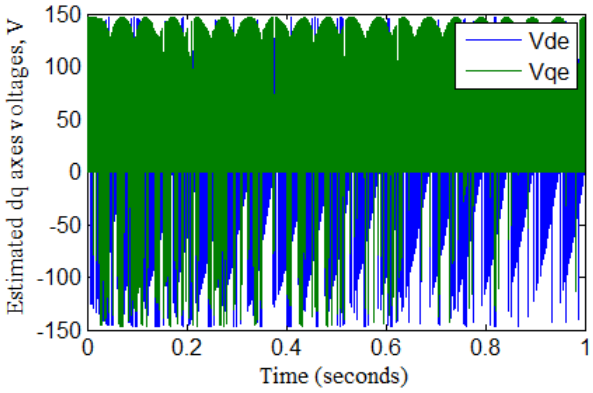

Fig. 7: Voltage vectors in estimated dq axes.

The actual current in estimated dq axes is shown in Fig. 9. Its fundamental and high frequency components are given in Fig. 10. The simulation for different reference idq currents are also carried out. It is found that there is enough high frequency component in the current responses even at zero current reference value.

The high frequency reactive power is shown in Fig. 11. The position error goes and settles to a very low value (steady state error) after the initial transients are over as shown in Fig. 12.

The estimated position with zero initial actual position angle is shown in Fig. 13. The position estimation for initial angle 30^o, 60^o and 90^o are shown in Fig. 14, Fig. 15 and Fig. 16 respectively. The position estimation converges to very low steady stater error in all the cases.

The position estimation with a negative step change in speed is given in Fig. 17. The estimated position follows the actual position even at speed transition. The estimated and actual speed is given in Fig. 18.

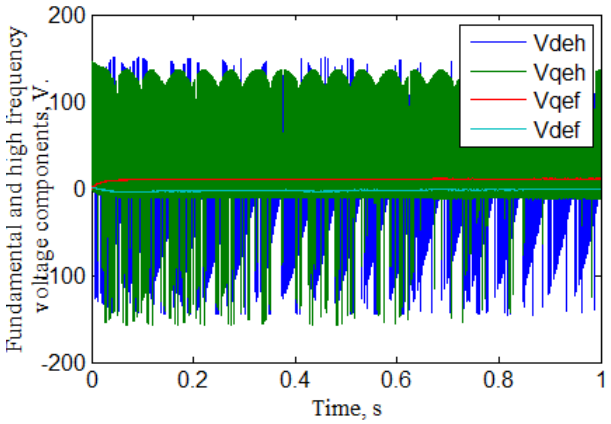

Fig. 8: High frequency and fundamental components of voltage vectors in estimated dq axes.

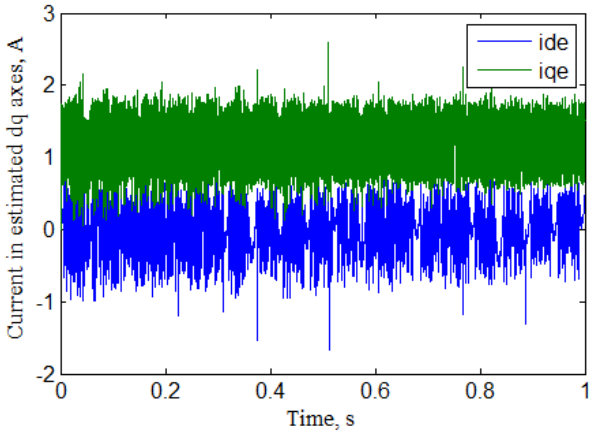

Fig. 9: Currents in estimated dq axes.

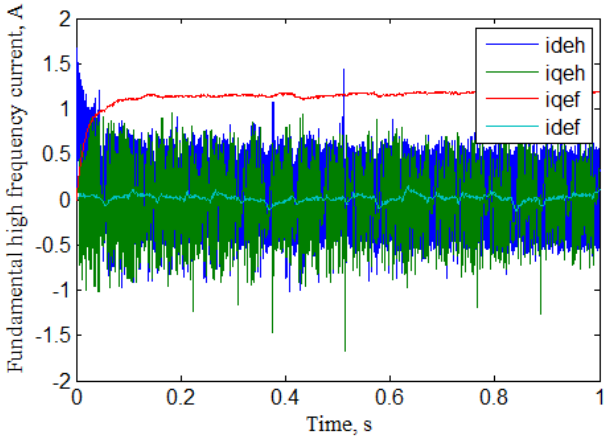

Fig. 10: High frequency and fundamental components of currents in estimated dq axes.

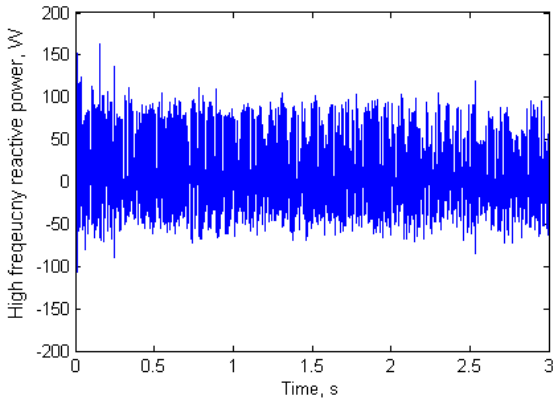

Fig. 11: High frequency reactive power.

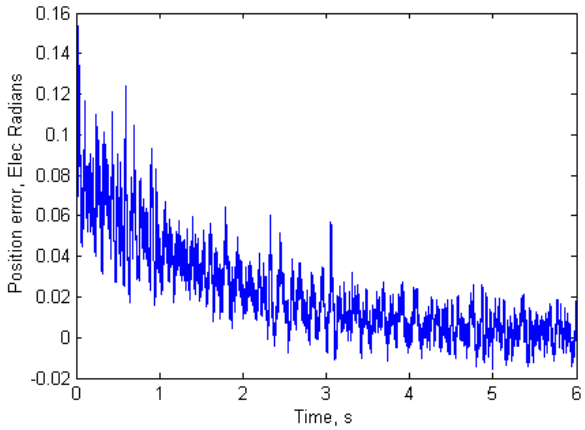

Fig. 12: Position error.

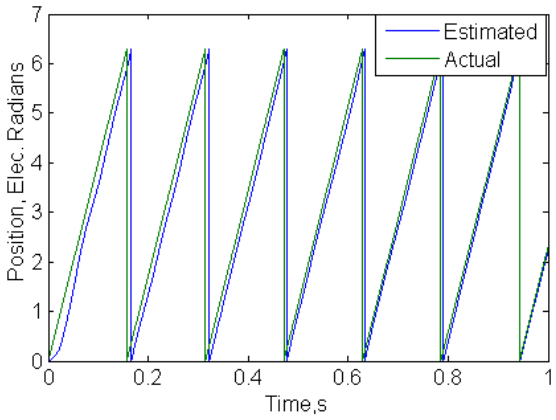

Fig. 13: Position estimation with zero initial position angle.

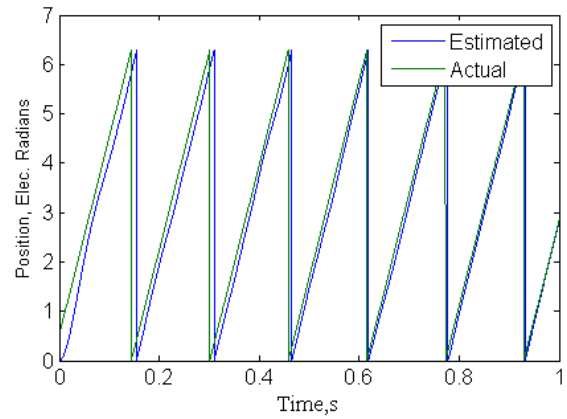

Fig. 14: Position estimation with 30^o initial position angle.

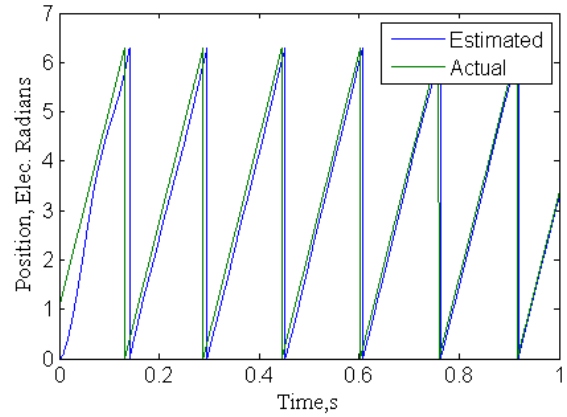

Fig. 15: Position estimation with 60^o initial position angle.

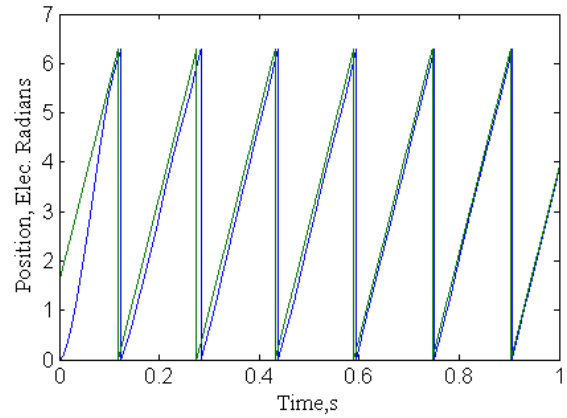

Fig. 16: Position estimation with 90^o initial position angle.

V. Conclusion

This paper presents position estimation scheme for IPM machine controlled by MPC with FCS. The inherent high frequency voltage vector injection of MPC with FCS is exploited to extract the position information. The high frequency current response is modulated with position. It is shown that MPC with FCS always have sufficient high frequency current component even at zero current reference. The demodulation technique by estimating high frequency reactive power is also proposed. The simulation results at various initial position confirm the validity of the proposed scheme. The next step of this work will be a thorough investigation of the proposed scheme by

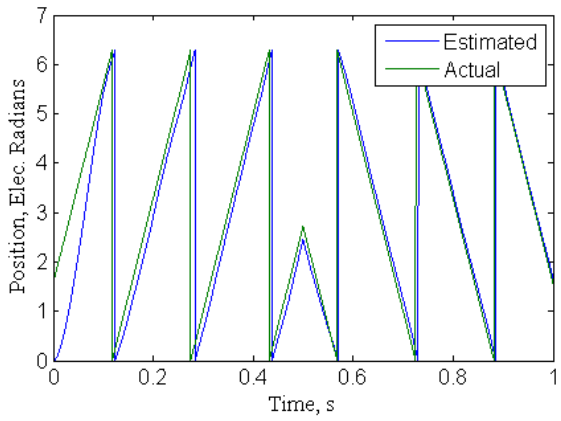

Fig. 17: Position estimation with a negative step change in speed.

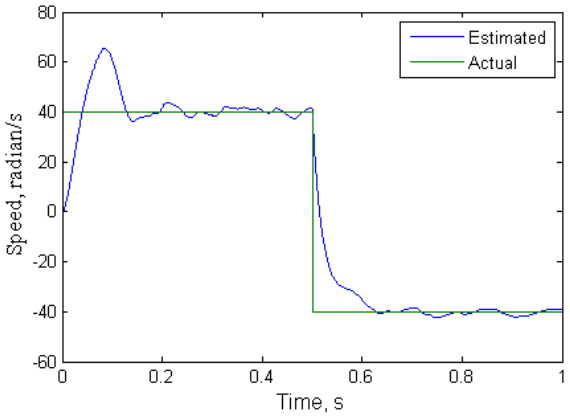

Fig. 18: Estimated and actual speed.

experiment in the entire operating region.

VI. Acknowledgment

This research was undertaken, in part, thanks to funding from the Canada Excellence Research Chairs Program.

References

[1] T. Geyer, "Generalized model predictive direct torque control: Long prediction horizons and minimization of switching losses," in *Proceedings of the IEEE Conference on Decision and Control*, pp.67996804. pp.

[2] M. Preindl and S. Bolognani, C. Danielson, "'Model Predictive Torque Control with PWM using fast gradient method, " in Twenty-Eighth Annual IEEE Applied Power Electronics Conference and Exposition (APEC), 2013, 25902597.

[3] M. Preindl and S. Bolognani, "Comparison of direct and PWM model predictive control for power electronic and drive systems," in Twenty-Eighth Annual IEEE Applied Power Electronics Conference and Exposition (APEC), 2103, pp.25262533.

[4] T. Geyer, "Computationally Efficient Model Predictive Direct Torque Control," *IEEE Trans. Power Electron.*, 2011, pp.28042816.

[5] T. Geyer, "Model Predictive Direct Torque Control: Derivation and Analysis of the State-Feedback Control Law," *IEEE Trans. Ind. Appl.*, 2013, pp.21462157.

[6] M. Preindl and S. Bolognani, "Model predictive direct speed control with finite control set of PMSM-VSI drive systems," in *Workshop on Predictive Control of Electrical Drives and Power Electronics,* Munich, 2011, pp. 17-23.

[7] M. Preindl and S. Bolognani, "Model predictive direct torque control with finite control set for PMSM drive systems, Part 1: Maximum torque per ampere operation," *IEEE Trans. Ind. Informat.*, pp.19121921.

[8] Liming Gong, " Carrier Signal Injection Based Sensorless Control of Permanent Magnet Brushless AC Machines"', PhD, dissertation, Dept. Electronics and Electrical Engineering., Univ. Sheffield, 2012.

[9] Y. Sun, M. Preindl, S. Sirouspour and A. Emadi, "Nonlinear modeling and design of initial position estimation and polarity detection of IPM drives," in 41st Annual Conference of the IEEE, *Industrial Electronics Society*, IECON, 2015, Yokohama, 2015, pp. 004059-004064.

[10] J. B. Bartolo, C. S. Staines and C. Caruana, "Flux position estimation using current derivatives for the sensorless control of AC machines," in *3rd International Symposium on Communications, Control and Signal Processing*, ISCCSP, 2008, pp. 1468-1473.

[11] A. Ravikumar Setty, S. Wekhande and K. Chatterjee, "Comparison of high frequency signal injection techniques for rotor position estimation at low speed to standstill of PMSM," in *IEEE 5th India International Conference on Power Electronics.* IICPE, Delhi, 2012, pp. 1-6.